Free Radical Biology & Medicine 52 (2012) 850–859

Contents lists available at SciVerse ScienceDirect

Free Radical Biology & Medicine

journal homepage: www.elsevier.com/locate/freeradbiomed

Original Contribution

Exploring real-time in vivo redox biology of developing and aging *Caenorhabditis elegans*

Patricia Back [a], Winnok H. De Vos [b], Geert G. Depuydt [a], Filip Matthijssens [a], Jacques R. Vanfleteren [a], Bart P. Braeckman [a,*]

[a] *Laboratory for Aging Physiology and Molecular Evolution, Department of Biology, Ghent University, 9000 Ghent, Belgium*
[b] *Bio-Imaging and Cytometry Unit, Department of Molecular Biotechnology, Ghent University, 9000 Ghent, Belgium*

ARTICLE INFO

Article history:
Received 31 March 2011
Revised 9 November 2011
Accepted 11 November 2011
Available online 23 December 2011

Keywords:
Caenorhabditis elegans
ROS
Redox balance
Biosensor
Aging
Dietary restriction
Development
Free radicals

ABSTRACT

Reactive oxygen species (ROS) are no longer considered merely toxic by-products of the oxidative metabolism. Tightly controlled concentrations of ROS and fluctuations in redox potential may be important mediators of signaling processes. Understanding the role of ROS and redox status in physiology, stress response, development, and aging requires their nondisruptive, spatiotemporal, real-time quantification in a living organism. We established *Caenorhabditis elegans* strains bearing the genetically encoded fluorescent biosensors HyPer and Grx1-roGFP2 for the detection of hydrogen peroxide (H_2O_2) and the glutathione redox potential, respectively. Although, given its transparency and genetic tractability, *C. elegans* is perfectly suitable as a model organism for such approaches, they have never been tried before in this nematode. We found that H_2O_2 treatment clearly induces a dose-dependent, reversible response of both biosensors in the living worms. The ratio of oxidized to reduced glutathione decreases during postembryonic development. H_2O_2 levels increase with age and this effect is delayed when life span is extended by dietary restriction. In young adults, we detected several regions with distinct redox properties that may be linked to their biological function. Our findings demonstrate that genetically encoded biosensors can reveal previously unknown details of in vivo redox biology in multicellular organisms.

Reactive oxygen species (ROS) were long considered as merely unwanted toxic by-products produced during oxidative metabolism, as they are tightly associated with aging and age-related diseases [1]. More recently, ROS were also found to be involved in proliferation, differentiation, immune response, and apoptosis [1–3]. In particular, hydrogen peroxide (H_2O_2) seems to be a key second messenger operating through reversible thiol oxidation in redox-sensitive proteins [4]. This is consistent with its stability and membrane permeativity, key features for intercellular signaling. ROS production influences redox status, which in turn affects development, senescence, and death. The glutathione redox potential provides an accurate proxy of the total redox state, because of the very high ratio of reduced glutathione (GSH) to oxidized glutathione (GSSG) and the high intracellular GSH abundance (1–11 mM) [5].

Because redox signaling acts through small and local changes, there is a need for sensitive, selective spatiotemporal measurements of H_2O_2 and GSH/GSSG in vivo. Most conventional redox-sensitive fluorogenic probes are nonspecific, irreversible, and disruptive [6]. Genetically encoded fluorescent sensors can overcome these limitations and have several advantages [7]. Whereas the suitability of externally added probes largely depends on how well they are taken up at the site of interest, any type of expression of genetically encoded sensors can be achieved using the appropriate promoter or signaling peptide. Over the past few years, much effort has been put into constructing redox-sensitive genetically encoded sensors [7]. The hydrogen peroxide-specific sensor HyPer is composed of a circularly permutated yellow fluorescent protein inserted into the H_2O_2-sensitive regulatory domain of the bacterial transcription factor OxyR (OxyR-RD) [8]. Selective and sensitive oxidation of HyPer by H_2O_2 generates a disulfide bridge between the separated parts of OxyR-RD, subsequently inducing changes in the fluorescent properties of the protein. These changes are reversible and quantified ratiometrically and are therefore independent of the HyPer expression level or photobleaching. HyPer is reduced in vivo by glutaredoxin-1 (Grx1) and GSH [9,10] and under normal physiological conditions this reduction is not limited by the GSH concentration [10]. Grx1-roGFP2, another ratiometric biosensor, specifically detects glutathione redox potential. The fusion of the human Grx1 to the redox-sensitive roGFP2 (redox-sensitive green fluorescent protein 2) greatly enhances the response to glutathione redox changes [11]. To conclude,

Abbreviations: DR, dietary restriction; Grx1-roGFP2, human glutaredoxin-1–redox-sensitive green fluorescent protein 2; GSH, reduced glutathione; GSSG, oxidized glutathione; INR, intensity-normalized ratio; LM, linear model; LMM, linear mixed model; ROS, reactive oxygen species; SOD, superoxide dismutase.

* Corresponding author. Fax: +32 9 264 87 93.
E-mail address: bart.braeckman@ugent.be (B.P. Braeckman).

0891-5849/$ – see front matter © 2011 Elsevier Inc. All rights reserved.
doi:10.1016/j.freeradbiomed.2011.11.037

oxidized-to-reduced ratios of HyPer and Grx1-roGFP2 can be used as proxies for H_2O_2 levels and GSSG/2GSH ratios, respectively.

In this study, we explored the redox biology of development and aging in the nematode *Caenorhabditis elegans* with these fluorescent probes. The use of this model in this particular research area has several advantages. *C. elegans* has an entirely transparent body, allowing the observation of spatiotemporal redox processes in vivo. Isogenic populations can be cultured in large synchronic populations and they develop and age in a short period of time [12].

Earlier studies in *C. elegans* suggest a role for ROS during development, oxidative stress response, and aging [13–15]. In *C. elegans* it was found that GSH concentration strongly declines during the adult life span [16] and the H_2O_2 production capacity of isolated mitochondria decreases with age [17]. However, all redox-related studies mentioned above have one major limitation: the redox-related measurements were not performed in vivo and therefore could not take into account the influence of the cellular and subcellular environment on ROS generation and detoxification. Neither could ROS be localized at the anatomical level. Using the genetically encoded sensors described above, we gained unprecedented insight in the topology and timing of redox signaling and oxidative stress in this model organism.

Materials and methods

Construction of HyPer and Grx1-roGFP2 transgenic strains

To obtain a constitutive and ubiquitous expression of the biosensors we performed a screen of the expression profiles of several annotated promoters (http://elegans.bcgsc.ca/perl/eprofile/index) and selected the promoter of a large ribosomal subunit L17 protein, *rpl-17*. HyPer from the mammalian pHyPer-Cyto vector (Evrogen) and Grx1-roGFP2 from the bacterial expression vector pQE-60 (a generous gift from T.P. Dick) were integrated into an expression vector with the ribosomal *rpl-17* promoter by MultiSite Gateway cloning [18] using pDONR 221 (Invitrogen), pDONR P4-P1R (Invitrogen), and pDEST-MB14 [19], devoid of GFP. *unc-119(ed3)* mutants were transformed with the HyPer or Grx1-roGFP2 expression vector containing *unc-119(+)* by microparticle bombardment using a Biolistic PDS-1000/He particle delivery system (Bio-Rad) [20]. All homozygous transgenic worms were backcrossed at least twice into N2 Bristol wild type (*jrIs1[Prpl-17::HyPer]*, *jrIs2[Prpl-17::Grx1-roGFP2]*).

Culture and sampling

Synchronous populations of the transgene and control strains were initiated from eggs prepared by alkaline hypochlorite treatment of gravid adults [21]. Worms were grown on cholesterol-supplemented nutrient agar (OXOID) plates containing a lawn of freshly grown *Escherichia coli* K12 cells. The nematode cultures used for external H_2O_2 stress experiments and confocal scanning were grown at 24 °C and sampled on the first day of egg laying. To examine the H_2O_2 levels and GSSG/2GSH ratios during postembryonic development, worms were cultured at 16 °C on agar plates seeded with K12. Larvae were sampled daily until they reached adulthood. Larval stage was determined with bright-field microscopy. Because large populations of nematodes were required for our fluorometric assays, we chose to culture synchronically aging cohorts in monoxenic liquid medium at 24 °C. This setup also enables the rigorous control of food supply needed to adequately induce dietary restriction (DR). The culture conditions we used in this study have been described previously and were clearly shown to induce a characteristic physiological aging phenotype [12,22]. By using an *hsp-16.2::GFP* reporter strain, we confirmed that 24 °C does not induce thermal stress (Supplementary Fig. S1). Synchronized L4 larvae, grown at 24 °C, were suspended in monoxenic liquid medium at densities not exceeding 2000 worms/ml. This medium contained S-buffer (43.55 mM KH_2PO_4, 6.45 mM K_2HPO_4, 100 mM NaCl, pH 6.0), 100 μM FUdR (to suppress reproduction), and frozen *E. coli* K12 cells (~3×10^9 cells/ml for fully fed conditions and ~8×10^8 cells/ml for dietary restriction). The dietary restriction bacterial concentration induced a maximal life-span extension. These liquid cultures were transferred to Fernbach flasks, incubated at 24 °C, and shaken at 120 rpm in a gyratory shaker incubator (New Brunswick Scientific, NJ, USA). Bacterial concentration in the culture was kept constant by measuring turbidity at 550 nm daily and K12 was added as needed. Samples were taken at adult day 1 and at ~50 and <25% survival. Juvenile stages were cultured different from adult stages for practical reasons: juveniles were grown at 16 °C on plate culture, because they develop more synchronously on plates. Culture temperature at 16 °C allowed sampling of one juvenile stage per day (light green bars in Fig. 2). Adults, on the other hand were grown in liquid at 24 °C (dark green bars in Fig. 2), thus allowing a better control of food supply and speeding up the aging process without stressing the worms. The samples harvested for fluorescence measurements were freed from dead worms, bacteria, and debris through Percoll and dense sucrose washing [23]. To remove the cuticular bacterial biofilm, the nematodes were washed with S-buffer containing 2.5 mM EDTA [24,25]. The resulting suspension of clean worms was used for spectrofluorometry and confocal microscopy.

Spectrofluorometry

Dense pellets of at least 1000 worms were loaded in a black, flat-bottom 96-well microtiter plate (Greiner, Frickenhausen, Germany). Fluorescence was measured for ~15 min at 25 °C with a Victor^2 1420 multilabel counter (PerkinElmer, Boston, MA, USA) with 490-nm (oxidized HyPer and reduced Grx1-roGFP2) and 405-nm (reduced HyPer and oxidized Grx1-roGFP2) excitation filters and a 535-nm emission filter. Unless otherwise noted, all data shown are averages of at least three biological repeats. For each biological repeat, at least three technical repeats were averaged over the time measured. The fluorescence for each technical repeat was normalized to protein content using the bicinchoninic acid (Pierce, Rockford, IL, USA) method. Corrections for autofluorescence in the transgenic strains were made by subtracting the 535-nm emission autofluorescence of matched wild types per protein content after 405- and 490-nm excitation, respectively, from that of HyPer or Grx1-roGFP2-expressing lines:

$$Oxidized/Reduced\ \ HyPer = \frac{\left[\left(\frac{HyPer\ \ Ex490Em535}{protein(mg)}\right)-\left(\frac{N2\ \ Ex490Em535}{protein(mg)}\right)\right]}{\left[\left(\frac{HyPer\ \ Ex405Em535}{protein(mg)}\right)-\left(\frac{N2\ \ Ex405Em535}{protein(mg)}\right)\right]}$$

$$Auto\,fluorescence = \frac{\left(\frac{HyPer\ \ Ex490Em535}{protein(mg)}\right)}{\left(\frac{HyPer\ \ Ex405Em535}{protein(mg)}\right)} - Oxidized/Reduced\ \ HyPer$$

For the quantification of oxidized/reduced Grx1-roGFP2 and fraction of autofluorescence, similar calculations were made with Ex405Em535 as the numerator and Ex490Em535 as denominator.

Confocal microscopy

For the anatomical localization of H_2O_2 levels and GSSG/2GSH ratios, we used a Nikon A1r confocal laser scanning microscopy system mounted on a Nikon Ti-E inverted epifluorescence microscope, equipped with a 405-nm diode laser and 488-nm multiline Ar laser. After treatment with 10 mM H_2O_2, HyPer transgenic worms were immobilized by being mounted on 2.5% agarose pads and scanned with a Plan Fluor 10×/0.5 objective, sequentially excited with both

laser lines (by line-scanning), set at minimal intensity to avoid ROS induction and bleaching, and detected through a 525/50 nm band-pass filter for 15 min at 1/4 fpm acquired at 30-s intervals. Transmitted light of the 488 line was captured simultaneously to obtain a bright-field image. To locate regions with distinct H_2O_2 or GSSG/2GSH steady-state levels, we paralyzed the worms with 10 mM tetramisole hydrochloride (levamisole; Sigma–Aldrich) and acquired high-resolution 3D images with a Plan Fluor 40×/1.3 immersion oil lens using the same optical configuration at a 256-Hz line frequency. Because of the time limitation within the experimental setup, it was technically impossible to scan the first 5 min after H_2O_2 addition. To quantify mean total H_2O_2 levels in old versus young adults, we scanned a mixed population of worms at their first and sixth day of adulthood with a Plan Fluor 10×/0.5 objective. We visualized, annotated, and quantified images with NIS-Elements 3.2 and Fiji, an open-source packaged version of ImageJ (W. Rasband, National Institutes of Health, Bethesda, MD, USA). *Z*-stacks of various neighboring regions were stitched to obtain a three-dimensional whole-organism montage of the worms. This was done for all three channels (405, 488, and transmission). Subsequently, stitched as well as individual fluorescence images were converted into intensity-normalized ratio (INR) images, hue saturation value images in which the hue represents the ratio of both fluorescence channels and the value the average intensity of both channels. With Fiji we measured the mean ratiometric values of various regions of interest over one or more selected optical slices of the stitched *Z*-stacks.

Statistical analysis

We performed general linear models (LM; PROC GLM) to test whether the HyPer and Grx1-roGFP2 ratios depend on the protein content in the samples (Supplementary Fig. S3). Linear mixed models (LMM; PROC MIXED) were used to assess whether fluorometric ratios change with time in both juveniles and adults. Furthermore, we investigated if changes in fluorometric ratio over time are affected by feeding conditions by including the variable feeding conditions and the two-way interaction in the model. As the same biological replicates were repeatedly measured over time, replicate was included as a random factor (RANDOM statement) and time was included as a repeated factor with replicate as subject term (REPEATED statement). Degrees of freedom were estimated following Kenward and Roger [26]. Assumptions of residual normality and homoscedasticity were satisfied and statistical analyses were performed in SAS 9.2. (SAS Institute, Inc., 2002–2003, Cary, NC, USA). To determine survival in aging cohorts, we daily scored the percentage of living worms (in 100 µl of twice-diluted culture suspension). Survival of populations was compared using the log rank tests in JMP 8.0.2 (SAS Institute, Inc., 2009). All results are represented by their mean ± standard error (SEM).

Results

In vivo response of HyPer and Grx1-roGFP2 transgenes to hydrogen peroxide treatment

We generated transgenic worms that express the biosensors HyPer and Grx1-roGFP2 constitutively in the cytosol under the promoter of the large ribosomal subunit 17. HyPer and Grx-1-roGFP2 fluorescence significantly exceeded background autofluorescence levels of age-matched wild types, except for the oxidized Grx1-roGFP2 fluorescence in old adults (Supplementary Fig. S2). The portions of autofluorescence were larger in Grx1-roGFP2 strains because the fluorescence levels of Grx1-roGFP2 were lower than those of HyPer transgenic worms. We confirmed that the steady-state fluorescence ratios of HyPer and Grx1-roGFP2 were independent of the protein content in the sample (Supplementary Fig. S3). Therefore, no normalization to biosensor protein is needed for these ratiometric measurements. Because the H_2O_2 detoxification capacity of homogenates of HyPer transgenic worms did not significantly differ from those of wild-type N2 ($P > 0.05$; unpaired *t* test; data not shown), we conclude that HyPer does not change the in vivo H_2O_2 steady-state levels.

As a proof of concept, we treated HyPer and Grx1-roGFP2 transgenic worms with hydrogen peroxide and we detected a fast, concentration-dependent, and reversible change in the fluorescence ratio in both transgenic strains (Fig. 1). We found that a minimal exogenous concentration of 0.5 mM H_2O_2 is needed to detect oxidation of HyPer. Lower concentrations did not yield any change in fluorescence properties of the worms. Addition of H_2O_2 caused a fast increase in the ratio of oxidized to reduced HyPer, reaching a maximum after about 10 min. At doses up to 10 mM, the worms' fluorescence ratio slowly returned to the initial steady-state levels in approximately 60 min (Fig. 1A). After this incubation period, the exogenous H_2O_2 was also depleted from the medium. No exogenous H_2O_2 was found in the medium as determined by absorbance at 240 nm (data not shown). Although less pronounced, the ratiometric increase in HyPer in individuals treated with 10 mM H_2O_2 was also found in the confocal scanning samples (Figs. 1B and C). This discrepancy may be inherent to the different protocols and equipment. First, worms observed with confocal microscopy were briefly treated with H_2O_2 after which they were transferred to agar pads devoid of H_2O_2, whereas worms measured in a spectrofluorometer were retained in S-buffer with H_2O_2. Second, there is a short time lapse of about 5 to10 min between the H_2O_2 treatment and the actual confocal scanning, so that we could resolve only the depletion part. Nevertheless, the kinetics detected with the confocal microscope correspond well with those measured in the fluorometer (half-life ~20 min).

H_2O_2 treatment (≥0.5 mM) triggers oxidation of Grx1-roGFP2 followed by reduction to initial steady-state levels (half-life ~15 min) (Fig. 1D). The response of HyPer and Grx1-roGFP2 to H_2O_2 is dose dependent (Figs. 1A and D). Worms stressed with H_2O_2 doses above 10 mM are incapable of reducing HyPer or Grx1-roGFP2 back to its initial steady-state level (Figs. 1A and D). Subsequent analysis on agar plates showed that these high doses were lethal to the worms under our experimental conditions (at least 1000 worms suspended in 100 µl S-buffer or M9 medium). The lethality threshold for H_2O_2 found in our study is similar to what was observed in another recent *C. elegans* study [15]. H_2O_2 addition initiated a stronger redox response of HyPer or Grx1-roGFP2 in cultures with low worm density, whereas in high-density cultures, H_2O_2 was detoxified faster (Supplementary Fig. S4). Therefore, we used constant worm densities in the experiment mentioned above (Figs. 1A and D). In vitro tests demonstrated that the fluorescence changes in HyPer and Grx1-roGFP2 upon H_2O_2 addition were truly reversible and do not represent the protein turnover of the probes [11] (Supplementary Fig. S5).

To test the sensitivity of the HyPer probe in vivo at a physiologically relevant level, we performed RNA inhibition of *ctl-1* and *ctl-2* on HyPer transgenic worms. We verified that the H_2O_2 detoxification capacity was reduced (Supplementary Fig. S6A). As expected, H_2O_2 levels were significantly increased in the *ctl* RNAi-treated strains ($P < 0.05$; unpaired *t* test; Supplementary Fig. S6B).

GSSG/2GSH ratios decrease exponentially during development

The development of *C. elegans* consists of an embryonic stage in the egg followed by four larval stages separated by molts. We measured HyPer and Grx1-roGFP2 fluorescence in synchronous postembryonic cohorts. No significant trend in H_2O_2 levels could be detected by linear regression analysis during larval development (Fig. 2A). It has been shown that changes in redox balance are associated with cell cycle and development [27]. In agreement with this finding, we detected a significant logarithmic decline in GSSG/2GSH ratios during larval development in Grx1-roGFP2 transgenic worms (Fig. 2B).

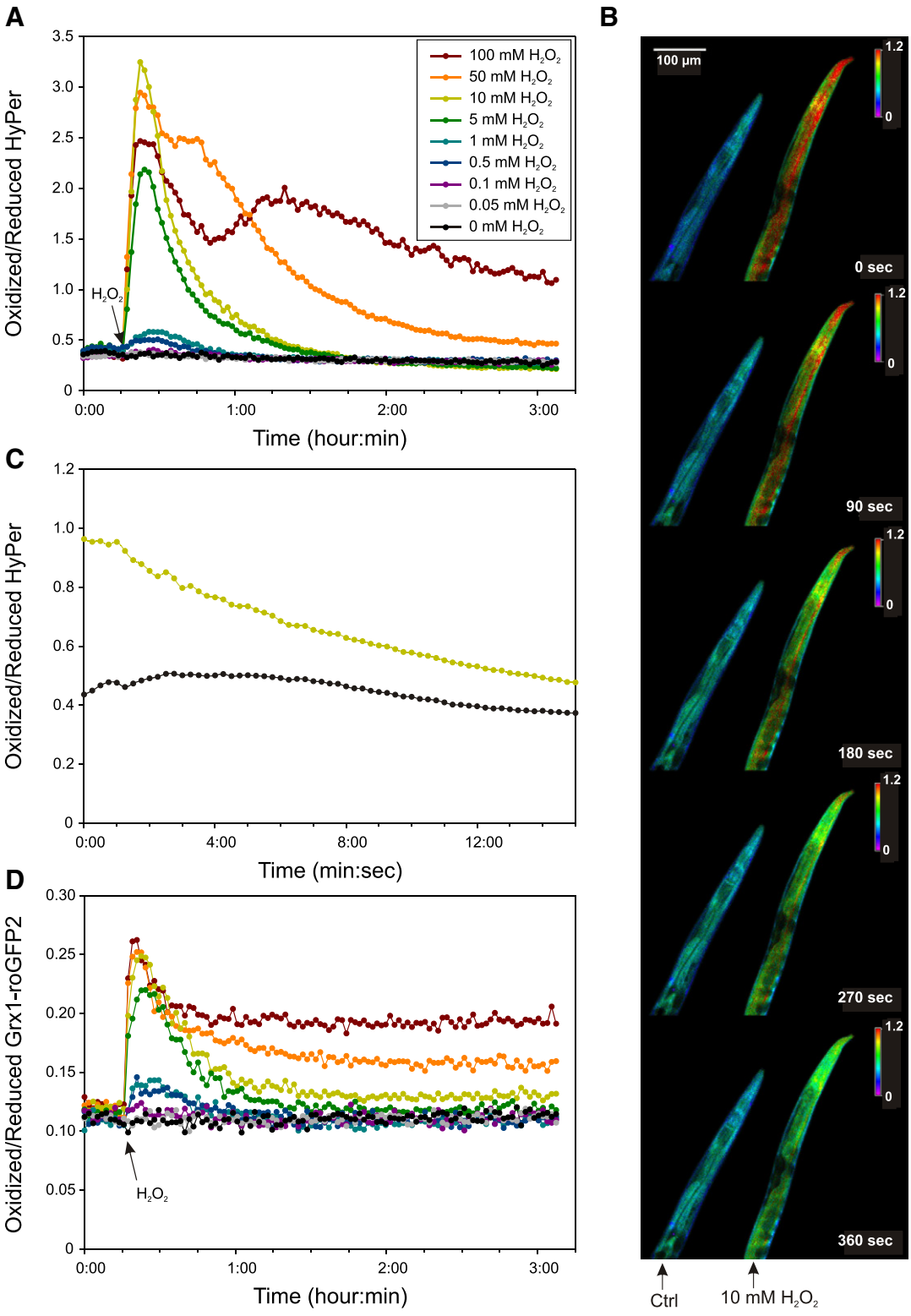

Fig. 1. In vivo HyPer response to exogenous H_2O_2 stress. (A) H_2O_2 treatment induces a transient dose-dependent increase in the ratio of oxidized to reduced HyPer in transgenic worms. The fluorescent transgenes were excited at 405 (reduced HyPer) and 490 nm (oxidized HyPer), and emission at 535 nm was quantified in a spectrofluorometer. Matched wild-type controls were used to correct for autofluorescence. (B) Intensity-normalized ratio images of an untreated (left) and a 10 mM H_2O_2-treated worm (right). The elevated H_2O_2 levels quickly disappear in the treated animal. (C) Quantification of the worm images shown in (B). Measurements were carried out as in (A). (D) In vivo Grx1-roGFP2 response to exogenous H_2O_2 stress. H_2O_2 induces a transient dose-dependent increase in the ratio of oxidized to reduced Grx1-roGFP2 in transgenic worms. Measurements were carried out as in (A), except that 405-nm excitation was used for oxidized Grx1-roGFP2 and 490 nm was used for reduced Grx1-roGFP2.

H_2O_2 levels increase with age

Oxidative damage accumulation is generally assumed to be a major cause of aging, although recently, its fundamental importance in aging has been questioned [28]. The understanding of the in vivo redox biology in aging organisms is of crucial importance to further evaluate this hypothesis. By using the HyPer and Grx1-roGFP2 biosensors in *C. elegans*, this goal can be achieved for the first time. We

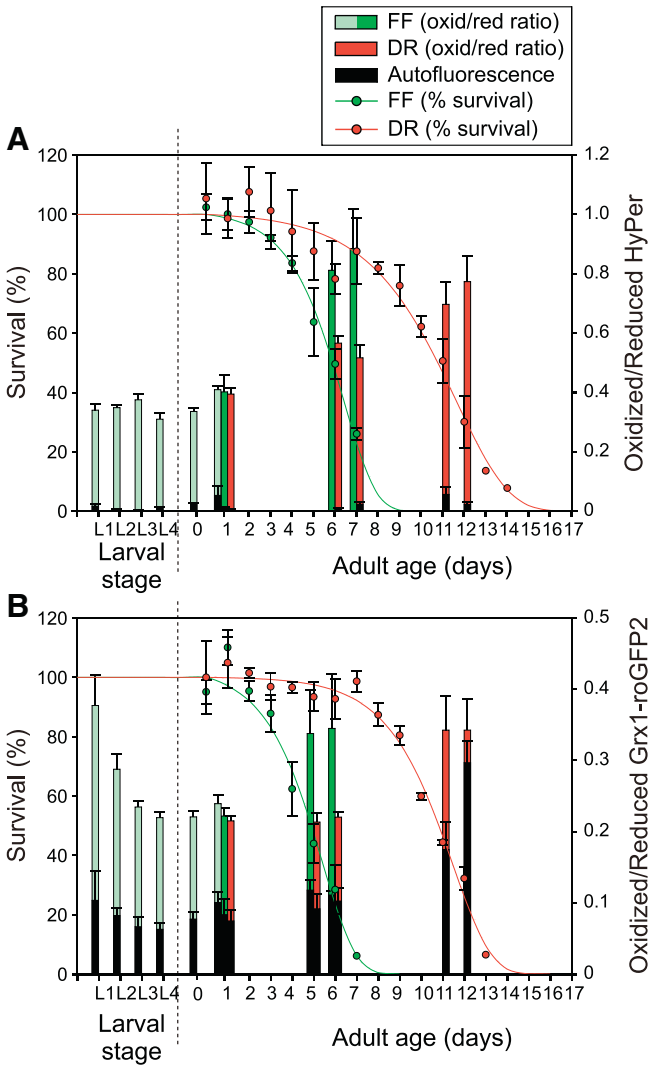

Fig. 2. (A) Survival (scatter plot with Gompertz fit) and H_2O_2 levels (stacked bars) during development and aging. Diet-restricted (DR) worms live 76% longer than fully fed (FF) HyPer transgenic worms ($P<0.0001$; log rank test). H_2O_2 levels did not change significantly during postembryonic development (L1–day 1; light green bars; slope $=0.0004\pm0.006$; $P=0.94$; LMM). H_2O_2 levels increase significantly with age in FF (dark green bars; slope $=0.083\pm0.028$; $P=0.0002$; LMM) and DR HyPer worms (red bars; slope $=0.030\pm0.009$; $P=0.005$). Although FF and DR worms have similar H_2O_2 levels at the first day of adulthood ($P=0.78$), DR significantly attenuated the age-related increase in H_2O_2 ($P=0.016$). The portion of autofluorescence in the total ratio value is indicated with black bars. Error bars represent SEM. (B) Survival (scatter plot with Gompertz fit) and GSSG/2GSH levels (stacked bars) during development and aging. The adult life of DR Grx1-roGFP2 transgenics is 116% longer than that of FF worms ($P<0.0001$; log rank test). GSSG/2GSH levels decrease logarithmically during postembryonic development (light green bars; slope $=-0.079\pm0.013$; $P<0.0001$; LMM). In adults, however, there is no significant linear increase in GSSG/2GSH ratios with age, because of large variance among biological replicates (dark green bars, FF, $P=0.15$; red bars, DR, $P=0.49$). No significant difference in linear trend could be found between the feeding conditions (DR vs FF; $P=0.13$). Note the substantial autofluorescence of the samples, as indicated with black bars. Error bars represent SEM.

first confirmed that the mean life spans of HyPer and Grx1-roGFP2 transgenic worms were largely comparable to those of N2 wild types, although the small differences in life span were significant (+11.3% for HyPer transgenic worms and −8.3% for Grx1-roGFP2 transgenic worms; $P<0.05$; log rank test; compared to N2) (Supplementary Fig. S7). The small differences in life span might be due to the biolistic transformation in the *unc-119(ed3)* background. Although we backcrossed the transgenic strains at least twice into N2 wild type, we cannot exclude that the transgenes are integrated in a genomic region that slightly influences life span. Nevertheless, we are primarily interested in the effect of a specific treatment, such as H_2O_2 addition, aging, and dietary restriction, on a specific transgenic strain.

We recently showed that ROS production capacity of isolated mitochondria decreases with age [17]. We wondered whether the in vivo H_2O_2 levels, depending on the balance between production and detoxification rates, would follow the same pattern. We observed that general HyPer fluorescence was reduced with age, but it still significantly exceeded the levels of autofluorescence, allowing accurate quantification of the ratio of oxidized to reduced HyPer (Supplementary Fig. S2). Using HyPer, we detected a significant increase in H_2O_2 levels with age (Fig. 2A).

The fluorescence data in Fig. 2 represent the average of a large synchronized population and do not take into account individual stochastic variation. Confocal scanning of individual young (day 0) and old (day 6) adults confirmed the spectrofluorometrical data but also showed a remarkable population heterogeneity in the H_2O_2 levels and distribution of old individuals (Figs. 3A and B).

Because GSH content was found to decrease with age [16] and previous human and mouse studies reported an age-related increase in the GSSG/2GSH ratio [29,30], we expected to find an increase in GSSG/2GSH ratio with age. However, we found in our Grx1-roGFP2-expressing strain that Grx1-roGFP2 fluorescence levels decrease with age, whereas the proportion of autofluorescence increases (Supplementary Fig. S2). Therefore, we were unable to obtain conclusive results for old worms, although Grx1-roGFP2 can clearly monitor GSSG/2GSH ratios in young populations (Fig. 2B).

Dietary restriction delays the age-dependent H_2O_2 increase

Reduction of bacterial density in monoxenic liquid culture from 3×10^9 to 8×10^8 cells/ml significantly prolongs mean and maximum life span of HyPer and Grx1-roGFP2 transgenic worms (Figs. 2A and B). This effect was similar to wild-type cultures (both $P>0.1$; log rank test; Supplementary Fig. S7). This DR regime is comparable with previous studies [31]. Decreasing the bacterial food supply doubles the life span (Supplementary Fig. S7), which implies that the controls are not calorie restricted. The restricted nematodes showed a morphology typical for calorie restriction (smaller body size, higher mobility, high transparency; Supplementary Fig. S8), and the controls had a well-fed phenotype (larger body size and darker gut).

Intracellular H_2O_2 levels, as measured with HyPer, significantly increased with age in dietary-restricted worms but at a slower rate compared to the fully fed controls (Fig. 2A). This resulted in similar H_2O_2 levels in DR and control worms at matched physiological age (100, 50, and 25% survival).

Local H_2O_2 hot spots in essential canal-associated neurons (CANs) and reduced GSH environment in spermatheca

HyPer and Grx1-roGFP2 transgenic worms were scanned with confocal microscopy on their first day of adulthood (designated day 0) to identify regions with distinct H_2O_2 levels or GSSG/2GSH ratios. The relative portion of autofluorescence was determined in matched N2 wild types under identical optical conditions and was negligible compared to the HyPer fluorescence. On the other hand, with the Grx1-roGFP2-specific microscope settings, we detected some autofluorescence in the intestine (Supplementary Fig. S9). Therefore, we excluded the intestine from ratiometric quantification in these experiments.

We measured the average ratio (ex 488/ex 405 em 525) of several regions of 3D-stitched HyPer transgenic adults. Within those regions with sufficiently high HyPer expression we detected several delineated areas with consistently deviating ratios such as head, body wall muscles, hyp7 (hypodermis), vulva, CAN, and tail (Fig. 4). Because HyPer expression is low in the intestine and the gonads the mean

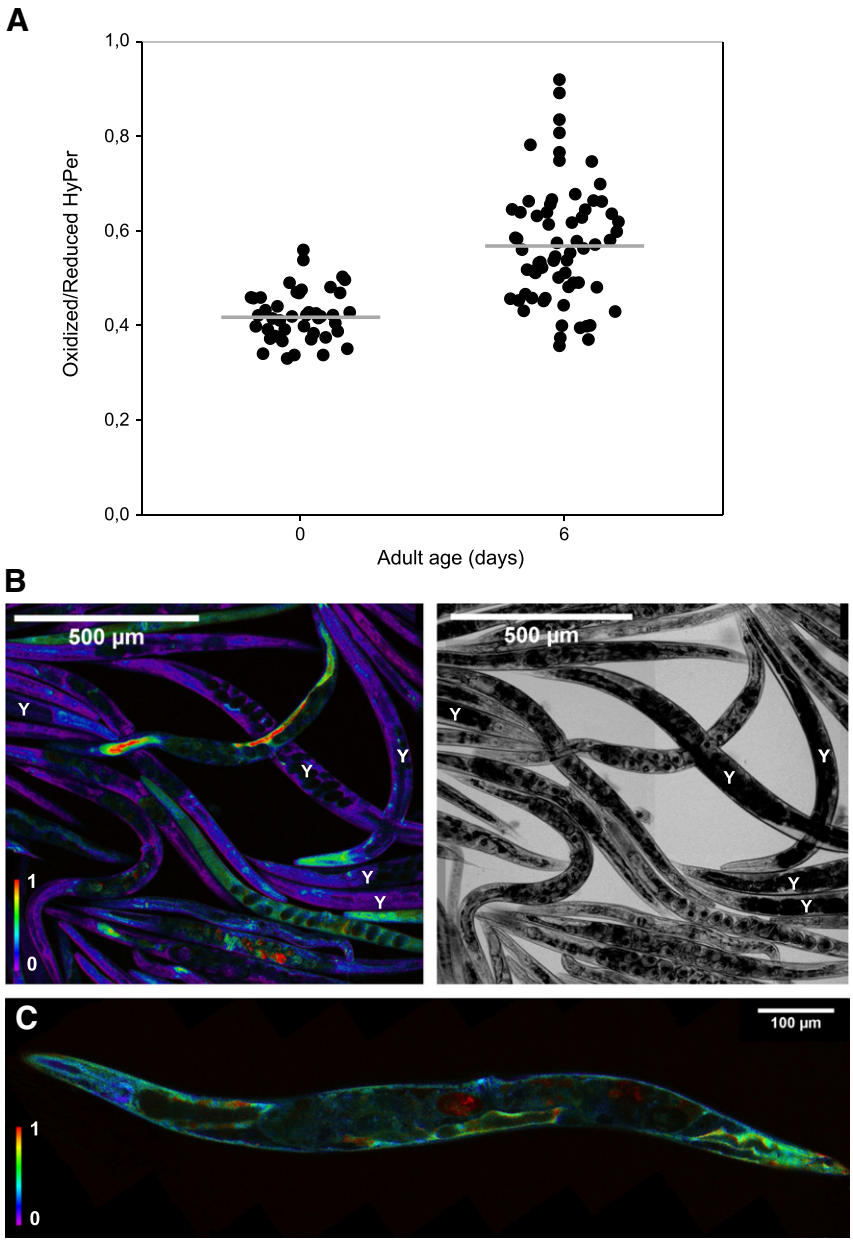

Fig. 3. Confocal analysis of young and old HyPer worms. (A) Dot plot of mean individual H_2O_2 levels of young (day 0) and old (day 6) adults scanned with the same laser settings and quantified over the whole worm body; the population mean is indicated by a horizontal line. H_2O_2 levels, averaged over the population, significantly increase with age. Day 0, 0.42 ± 0.008; day 6, 0.57 ± 0.016; $P<0.01$ (paired t test). (B) INR and confocal transmission images of a mixed population of young (Y) and old HyPer transgenic worms (not labeled). (C) INR false-colored image of one Z-level of a 3D-stitched 6-day-old worm. Calibration bars in the INR images indicate the ratio of 525-nm emission after excitation at 488 nm vs 405 nm. Because of the different laser settings, which were optimized for scanning the old worms, the ratio values of the old worm (C) should not be directly compared to those of the young worms in Fig. 4.

ratio of the selected regions was compared with that of the integral nematode, intestine and gonads excluded. The low HyPer expression in gonads may be due to transgene silencing [32].

H_2O_2 levels in canal-associated neurons (CANL and CANR) were significantly higher compared to other tissues (Figs. 4A and D). CAN identity was verified by comparison with the *otIs85[srq-1::gfp;rol-6(d)]* transgenic strain expressing GFP in the CAN cells specifically (Supplementary Fig. S10). The hypodermal syncytium, hyp7, contains significantly elevated H_2O_2 steady-state levels (Figs. 4B and D). Remarkably, we noted high H_2O_2 levels in the hyp7 nucleoplasm (Fig. 4B). The biological significance of this pattern remains obscure, although it may suggest a possible role for H_2O_2 signaling in hypodermal transcription. H_2O_2 levels in the body wall muscles were significantly raised as well (Figs. 4B and D). In contrast, we did not detect increased H_2O_2 levels in the pharynx (Figs. 4C and D). Further, we observed high H_2O_2 amounts in interfacial epithelial cells lining the pharyngeal buccal cavity, the vulva, and especially the rectum (tail section), although these elevations did not reach significance (Figs. 4C and D). Six-day-old adults did not show these spatial H_2O_2 patterns (Fig. 3C). In the CANs, hyp7, and body wall muscles of old worms, H_2O_2 levels were not significantly raised. Occasionally, we found high H_2O_2 levels in dead embryos inside old FUdR-treated worms.

We quantified the average GSSG/2GSH ratio (ex 405/ex 488 em 525/50) in the head, tail, and spermatheca of several Grx1-roGFP2 day 0 adults (Fig. 5B). These averaged ratios were compared with the ratio of the entire worm without the intestine (high autofluorescence, Supplementary Fig. S9) or gonads (low biosensor expression). The spermathecae, which are sites of oocyte fertilization, showed significantly

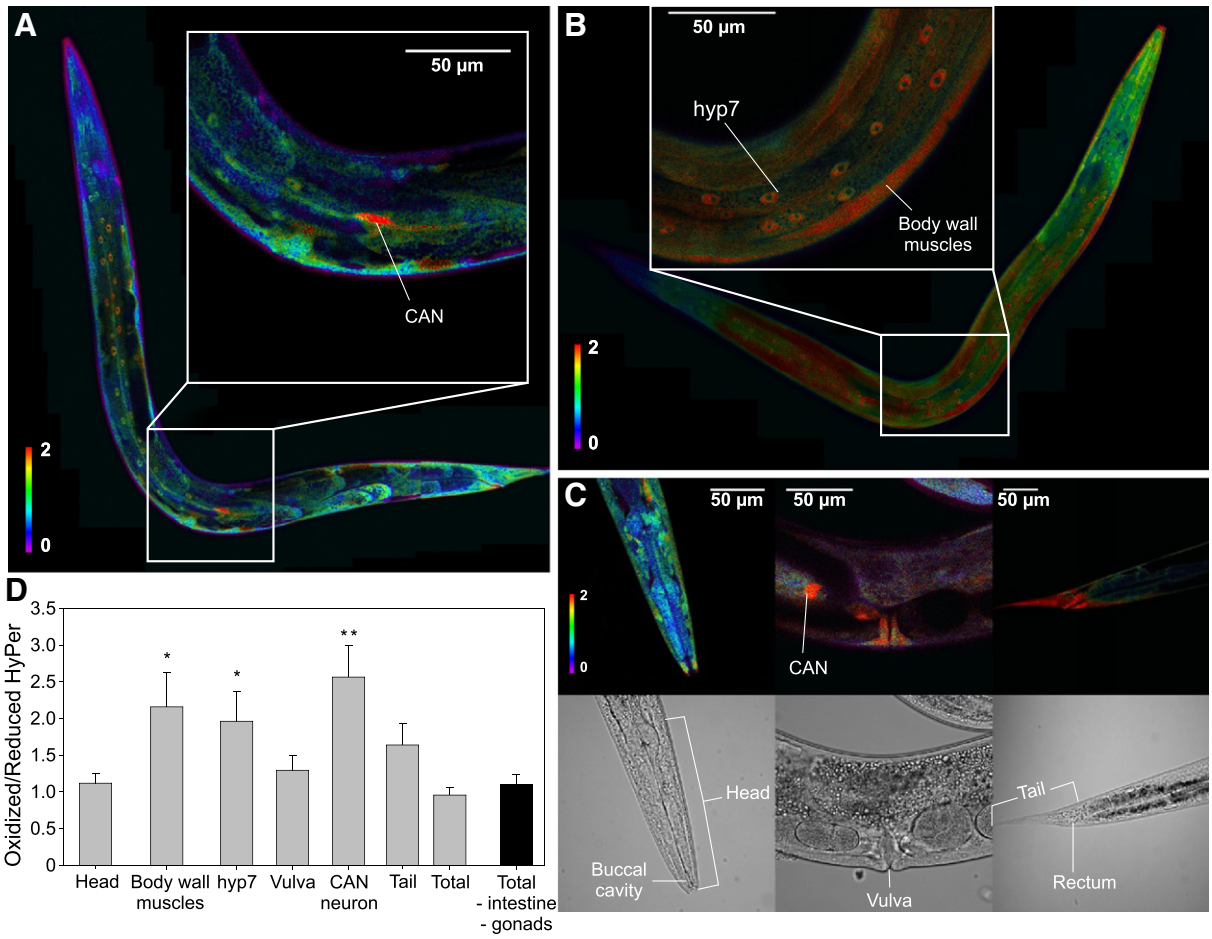

Fig. 4. Spatial patterns of H_2O_2 levels in young HyPer transgenic adults (first day of adulthood). (A) In the INR false-colored image of one *Z*-level of 3D-stitched worms, the high H_2O_2 levels are clearly visible in the CAN. (B) High H_2O_2 levels were also observed in the nucleoplasm of the hypodermal syncytium and in the body wall muscles. (C) INR and confocal transmission images of head, vulva, and tail region. Calibration bars in the INR images indicate the ratio of 525-nm emission after excitation at 488 nm vs 405 nm. (D) Ratiometric quantification of several regions of young (first day of adulthood) integral, 3D-stitched HyPer transgenes (pattern consistency was verified in 36 animals; 9 representative animals were used for 3D stitching and quantification). Error bars represent SEM; $^*P<0.05$; $^{**}P<0.01$ (paired *t* test, total − gut − gonads compared).

reduced GSSG/2GSH ratios (Figs. 5A and B). Other body regions did not differ significantly from the mean, suggesting that GSSG/2GSH redox status is kept fairly constant throughout the *C. elegans* body.

Discussion

Intracellular redox changes, associated with proliferation, differentiation, senescence, and death, are influenced by H_2O_2 steady-state levels and GSH redox potential in cell cultures [1,5]. In this study, we monitored these parameters for the first time in vivo in a multicellular organism during its developmental and aging process.

We found a rapid and reversible change in H_2O_2 levels and GSSG/2GSH ratios upon H_2O_2 administration. The lowest dose of exogenous H_2O_2 that elicited a detectable biosensor response was close to 0.5 mM. In contrast, a concentration as low as 5 µM H_2O_2 could activate OxyR in *E. coli* cells or induce a transient fluorescence change in HyPer in HeLa cell cultures [8,9]. This large difference between detection limits is probably due to the *C. elegans* cuticle, which is a highly impervious barrier isolating the worm from its environment. Our confocal images are indeed consistent with H_2O_2 being taken up mainly by the alimentary system and not by diffusion through the cuticle (Fig. 1B). The HyPer fluorescence kinetics of H_2O_2 detoxification are comparable to the kinetics of OxyR found in vitro and in *E. coli* cells [9]. Likewise, the kinetics of the H_2O_2-mediated Grx1-roGFP2 response in *C. elegans* are comparable to the changes described in yeast and *Arabidopsis* but much slower than those in HeLa cells [11,33,34]. This may be due to a suboptimal function of the human Grx-1 moiety of the biosensor in nonhuman cells.

The well-documented influence of ROS and redox status on in vitro proliferation, differentiation, migration, and cell death [3] suggests a role for ROS in development. Therefore, we quantified the in vivo H_2O_2 levels during postembryonic development but we did not find any clear change over time. As our measurements were performed on large synchronous worm populations we cannot exclude the occurrence of more subtle changes in particular cells or tissues of individuals during development. In contrast, the GSSG/2GSH ratios decreased logarithmically throughout larval development. Differentiating cells are characterized by a high GSSG/2GSH reduction potential [5] and during the first three larval stages, the number of differentiating cells in *C. elegans* decreases [35]. This may explain the clear decreasing trend of GSSG/2GSH ratios observed over the first three larval stages. It was shown in mammalian studies that GSH content increases during gametogenesis [36]. Because gametogenesis in *C. elegans* occurs at the L3/L4 molt, this matches with the decreasing GSSG/2GSH ratios measured during the L3 to L4 transition in our experiments (Fig. 2B).

Fifty years after the postulation of the free radical theory of aging, the role of ROS in the aging process remains inconclusive. For example, deletion or overexpression of the ROS detoxification enzyme SOD has little to no effect on life span in *C. elegans* [28]. In *C. elegans*, metabolic rate (respiration, heat production, and ATP levels) and antioxidant activity (SOD, H_2O_2 removal capacity, GSH concentration,

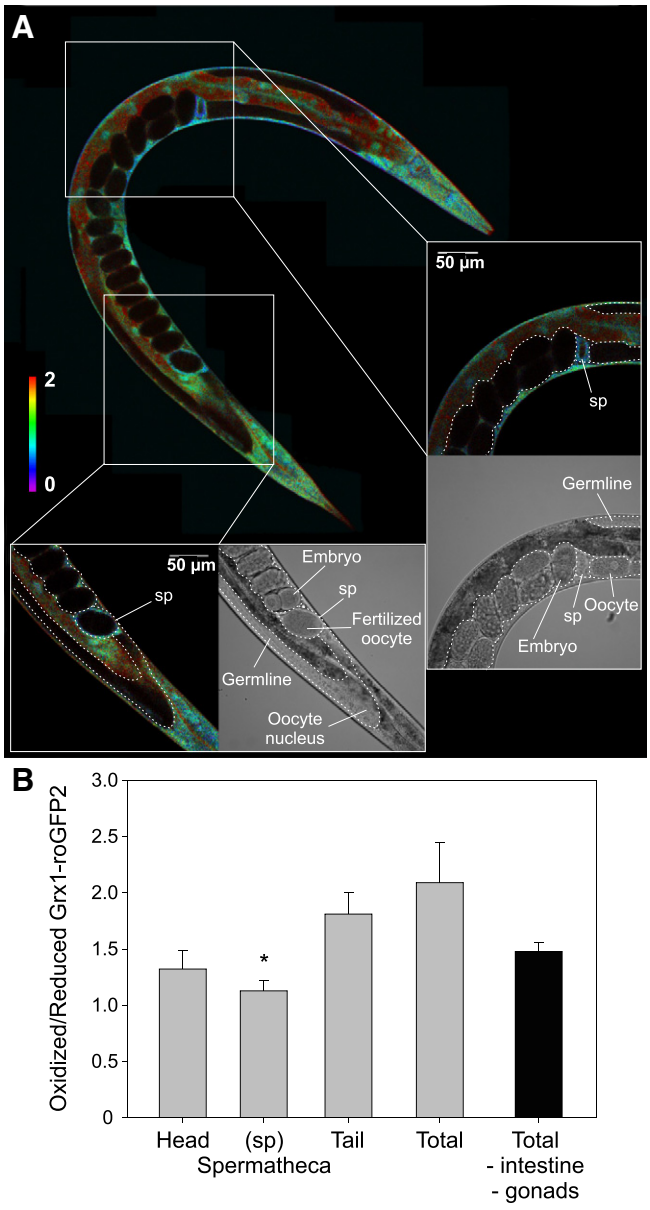

Fig. 5. Spatial patterns of GSSG/2GSH ratios in young (first day of adulthood) Grx1-roGFP2 transgenic adults. (A) INR false-colored image of one *Z*-level of 3D-stitched worms. The anterior and posterior spermathecae (sp) show low GSSG/2GSH ratios. Calibration bar indicates the ratio of 525-nm emission after excitation at 405 nm vs 488 nm. (B) Quantification of Grx1-roGFP2 as in Fig. 4D (pattern consistency was verified in 15 animals, 4 representative animals were 3D stitched and quantified). Error bars represent SEM; $^*P<0.05$ (paired *t* test, total − gut − gonads compared).

bioreduction capacity) decline with age [14]. Counterintuitively, the ROS production capacity decreases in isolated mitochondria [17] and carbonylated proteins tend to accumulate [37]. Therefore, the increase in H_2O_2 levels with age (Fig. 2A) suggests a diminished H_2O_2 detoxification rather than enhanced H_2O_2 production during aging. Confocal scanning of an old synchronized population revealed a large variation in individual H_2O_2 levels (Figs. 3A and B). This heterogeneity was also observed in the mobility decline [38] and autofluorescence increase [39] in synchronized aging populations. It would be interesting to investigate whether a correlation exists between these phenotypes and H_2O_2 levels in individuals. Like most sensors based on circularly permutated yellow fluorescent proteins, HyPer fluorescence depends on pH [8]. The nematode intestine becomes slightly acidified with increasing age (K. Nehrke, personal communication). Because acidification reduces the ratio of oxidized vs reduced HyPer, the higher levels of oxidation during aging that we report may be underestimated. Because HyPer fluorescence is very low in the intestine, this underestimation will be rather small.

Reducing dietary intake, without malnutrition, delays aging and extends life span in a wide variety of species [40], including *C. elegans* [31]. Despite numerous studies, it is still not clear which biochemical mechanism(s) is responsible for life-span extension under DR conditions. It is suggested that increased ROS formation that was observed upon DR would activate the antioxidant defense system [41]. Indeed, increased activity of SOD and catalase under DR has been reported [14,41]. We found that dietary restriction delays the increase in H_2O_2 with age. Consistent with mitohormetic life-span extension during DR, our results could indicate that although ROS production rates are increased upon DR [41], these ROS are extensively detoxified by an overcompensating antioxidant response.

We were interested in identifying distinct anatomical patterns of H_2O_2 levels or GSSG/2GSH ratios, as local differences may reveal a role of ROS or redox status in site-specific signaling. CANs showed strongly elevated H_2O_2 levels. These neurons, together with pharyngeal M4 neurons, are the only neurons of 302 that are essential for *C. elegans* development [42]. The CANs are tightly associated with the canals of the excretory cell, and laser ablation of these neurons results in dead clear larvae [43]. Accumulation of fluid in the pseudocoelom of these larvae suggests that CANs influence the excretory cells and thus osmoregulation. The extremely high levels of H_2O_2 in CANs may be a signaling cue for osmoregulation.

Together with the hypodermal syncytium, hyp7, several interfacial epithelial cells also had relatively high H_2O_2 levels. These epithelial cells secrete the cuticle, which is predominantly composed of collagens and cuticulins. Ce-Duox1 (and possibly Ce-Duox2), exclusively expressed in hypodermal cells, generates H_2O_2 and catalyzes the H_2O_2-mediated tyrosine cross-linking between collagens and cuticulins [44]. These cross-links are essential for the strength and integrity of the cuticle [45], and loss of Ce-Duox1 induces blister formation [44]. As collagen synthesis continues after maturation [38], it is probable that we were able to detect elevated H_2O_2 levels in the cuticle-secreting cells of adult worms.

The high H_2O_2 levels in body wall muscle could be a side effect of the levamisole-induced paralysis that is necessary for confocal microscopy of live worms. Levamisole is a specific acetylcholine receptor agonist of the body wall muscle cells [46] causing body wall tetanus, but not pharyngeal tetanus [47]. Studies have demonstrated that, in mice, muscle contraction can increase H_2O_2 production [48]. Indeed, we found increased H_2O_2 levels only in the body wall, not in the pharynx (Figs. 4C and D). The use of agar pads for immobilization may avoid this artifact but worms mounted on agar pads dry out very fast, and therefore it makes the slow process of detailed confocal scanning for localizing H_2O_2 patterns technically challenging.

We could not detect these clear spatial H_2O_2 patterns in old individuals (Fig. 3D). In old worms, these patterns were heterogeneous and seemed more randomly distributed throughout the worm body. However, the overall HyPer ratio was increased. It seems that during aging the H_2O_2 levels increase globally rather than locally. This may infer that, in old worms, increased H_2O_2 levels are not characterized by a fixed spatiotemporal pattern that drives a unique sequence of aging-related events. It is likely that, because of this stochastic variation, individual worms may show different aging rates in different tissues.

Spermathecae showed conspicuously low GSSG/2GSH ratios. In mammals, GSH synthesis is increased during gametogenesis and fertilization in gametes [49] as well as the surrounding tissue [50], most probably for protection against oxidative stress [36,49]. Our images suggested that this feature may be evolutionarily conserved (Fig. 5). Moreover, in *C. elegans,* the glutathione *S*-transferases *gst-4* and *gst-1* are necessary for sperm maintenance in the spermatheca and therefore required for fertilization [51]. We also noticed low

total GSSG/2GSH ratios during the fourth larval stage (Fig. 2B), when spermathecae are generated and sperm mature.

In general, we found that regions with distinct H_2O_2 levels did not correspond to those with high or low GSSG/2GSH ratios. This may reflect that H_2O_2 is neither directly nor exclusively detoxified by GSH and that expression patterns of the different H_2O_2-detoxifying enzymes may vary.

In conclusion, H_2O_2 treatment induced a rapid, reversible, and dose-dependent in vivo response of HyPer and Grx1-roGFP2. During postembryonic development, GSSG/2GSH ratios decreased logarithmically whereas the increase in H_2O_2 levels during aging was delayed under diet-restricted conditions. In young adults we could identify local regions with high H_2O_2 levels and low GSSG/2GSH ratios, which are probably related to their function in osmoregulation, cuticle formation, and fertilization. With this study, in vivo redox biosensors were successfully used for the first time in the model organism *C. elegans* thereby revealing novel aspects in redox biology during development and aging.

Supplementary materials related to this article can be found online at doi:10.1016/j.freeradbiomed.2011.11.037.

Acknowledgments

The *otIs85[srq-1::gfp;rol-6(d)]* transgenic strain was kindly provided by the *Caenorhabditis* Genetics Center. Grx1-roGFP2 in the bacterial expression vector pQE-60 was kindly provided by T.P. Dick. We acknowledge Marjolein Couvreur for the microinjection of transgenes, Greet De Coster for assistance with the statistical analyses, and Filip Matthijssens for the useful comments and discussion on the manuscript. This work was supported by grants from the European Community (LSHM-CT-2004-512020) and the Fund for Scientific Research–Flanders (G.0025.06) to J.R.V. and B.P.B. P.B. acknowledges a Ph.D. grant from the Institute for the Promotion of Innovation through Science and Technology in Flanders (IWT-Vlaanderen). NB-photonics and financial support from the Hercules Foundation (Project AUGE/013) are gratefully acknowledged.

References

[1] Droge, W. Free radicals in the physiological control of cell function. *Physiol. Rev.* **82:**47–95; 2002.
[2] Finkel, T.; Holbrook, N. J. Oxidants, oxidative stress and the biology of ageing. *Nature* **408:**239–247; 2000.
[3] Hernandez-Garcia, D.; Wood, C. D.; Castro-Obregon, S.; Covarrubias, L. Reactive oxygen species: a radical role in development? *Free Radic. Biol. Med.* **49:** 130–143; 2010.
[4] Veal, E. A.; Day, A. M.; Morgan, B. A. Hydrogen peroxide sensing and signaling. *Mol. Cell* **26:**1–14; 2007.
[5] Schafer, F. Q.; Buettner, G. R. Redox environment of the cell as viewed through the redox state of the glutathione disulfide/glutathione couple. *Free Radic. Biol. Med.* **30:**1191–1212; 2001.
[6] Gomes, A.; Fernandes, E.; Lima, J. L. Fluorescence probes used for detection of reactive oxygen species. *J. Biochem. Biophys. Methods* **65:**45–80; 2005.
[7] Meyer, A. J.; Dick, T. P. Fluorescent protein-based redox probes. *Antioxid. Redox Signal.* **13:**621–650; 2010.
[8] Belousov, V. V.; Fradkov, A. F.; Lukyanov, K. A.; Staroverov, D. B.; Shakhbazov, K. S.; Terskikh, A. V.; Lukyanov, S. Genetically encoded fluorescent indicator for intracellular hydrogen peroxide. *Nat. Methods* **3:**281–286; 2006.
[9] Aslund, F.; Zheng, M.; Beckwith, J.; Storz, G. Regulation of the OxyR transcription factor by hydrogen peroxide and the cellular thiol–disulfide status. *Proc. Natl. Acad. Sci. U. S. A.* **96:**6161–6165; 1999.
[10] Zheng, M.; Aslund, F.; Storz, G. Activation of the OxyR transcription factor by reversible disulfide bond formation. *Science* **279:**1718–1721; 1998.
[11] Gutscher, M.; Pauleau, A. L.; Marty, L.; Brach, T.; Wabnitz, G. H.; Samstag, Y.; Meyer, A. J.; Dick, T. P. Real-time imaging of the intracellular glutathione redox potential. *Nat. Methods* **5:**553–559; 2008.
[12] Braeckman, B. P.; Houthoofd, K.; De Vreese, A.; Vanfleteren, J. R. Assaying metabolic activity in ageing *Caenorhabditis elegans*. *Mech. Ageing Dev.* **123:**105–119; 2002.
[13] Shibata, Y.; Branicky, R.; Landaverde, I. O.; Hekimi, S. Redox regulation of germline and vulval development in *Caenorhabditis elegans*. *Science* **302:**1779–1782; 2003.
[14] Houthoofd, K.; Braeckman, B. P.; Lenaerts, I.; Brys, K.; De Vreese, A.; Van Eygen, S.; Vanfleteren, J. R. No reduction of metabolic rate in food restricted *Caenorhabditis elegans*. *Exp. Gerontol.* **37:**1359–1369; 2002.
[15] Kumsta, C.; Thamsen, M.; Jakob, U. Effects of oxidative stress on behavior, physiology, and the redox thiol proteome of *Caenorhabditis elegans*. *Antioxid. Redox Signal.* **14:** 1023–1037; 2011.
[16] Brys, K.; Vanfleteren, J. R.; Braeckman, B. P. Testing the rate-of-living/oxidative damage theory of aging in the nematode model *Caenorhabditis elegans*. *Exp. Gerontol.* **42:**845–851; 2007.
[17] Brys, K.; Castelein, N.; Matthijssens, F.; Vanfleteren, J. R.; Braeckman, B. P. Disruption of insulin signalling preserves bioenergetic competence of mitochondria in ageing *Caenorhabditis elegans*. *BMC Biol.* **8:**91; 2010.
[18] Magnani, E.; Bartling, L.; Hake, S. From Gateway to Multisite Gateway in one recombination event. *BMC Mol. Biol.* **7:**46; 2006.
[19] Dupuy, D.; Li, Q. R.; Deplancke, B.; Boxem, M.; Hao, T.; Lamesch, P.; Sequerra, R.; Bosak, S.; Doucette-Stamm, L.; Hope, I. A.; Hill, D. E.; Walhout, A. J. M.; Vidal, M. A first version of the *Caenorhabditis elegans* Promoterone. *Genome Res.* **14:** 2169–2175; 2004.
[20] Praitis, V.; Casey, E.; Collar, D.; Austin, J. Creation of low-copy integrated transgenic lines in *Caenorhabditis elegans*. *Genetics* **157:**1217–1226; 2001.
[21] Sulston, J. E.; Hodgkin, J. The Nematode *Caenorhabditis elegans*. Cold Spring Harbor Laboratory Press, Cold Spring Harbor, NY; 1988.
[22] Braeckman, B. P.; Houthoofd, K.; Vanfleteren, J. R. Assessing metabolic activity in aging *Caenorhabditis elegans*: concepts and controversies. *Aging Cell* **1:**82–88 discussion 102-103; 2002.
[23] Fabian, T. J.; Johnson, T. E. Production of age-synchronous mass cultures of *Caenorhabditis elegans*. *J. Gerontol.* **49:**B145–156; 1994.
[24] Rao, A. U.; Carta, L. K.; Lesuisse, E.; Hamza, I. Lack of Herne synthesis in a free-living eukaryote. *Proc. Natl. Acad. Sci. U. S. A.* **102:**4270–4275; 2005.
[25] Yuan, Z.; VanBriesen, J. M. Bacterial growth yields on EDTA, NTA, and their biodegradation intermediates. *Biodegradation* **19:**41–52; 2008.
[26] Kenward, M. G.; Roger, J. H. Small sample inference for fixed effects from restricted maximum likelihood. *Biometrics* **53:**983–997; 1997.
[27] Allen, R. G.; Balin, A. K. Oxidative influence on development and differentiation: an overview of a free radical theory of development. *Free Radic. Biol. Med.* **6:** 631–661; 1989.
[28] Gems, D.; Doonan, R. Antioxidant defense and aging in *C. elegans*: is the oxidative damage theory of aging wrong? *Cell Cycle* **8:**1681–1687; 2009.
[29] Droge, W. Oxidative stress and ageing: is ageing a cysteine deficiency syndrome? *Philos. Trans. R. Soc. Lond. B Biol. Sci.* **360:**2355–2372; 2005.
[30] Rebrin, I.; Forster, M. J.; Sohal, R. S. Effects of age and caloric intake on glutathione redox state in different brain regions of C57BL/6 and DBA/2 mice. *Brain Res.* **1127:** 10–18; 2007.
[31] Klass, M. R. Aging in the nematode *Caenorhabditis elegans*: major biological and environmental factors influencing life span. *Mech. Ageing Dev.* **6:**413–429; 1977.
[32] Kelly, W. G.; Fire, A. Chromatin silencing and the maintenance of a functional germline in *Caenorhabditis elegans*. *Development* **125:**2451–2456; 1998.
[33] Marty, L.; Siala, W.; Schwarzlander, M.; Fricker, M. D.; Wirtz, M.; Sweetlove, L. J.; Meyer, Y.; Meyer, A. J.; Reichheld, J. P.; Hell, R. The NADPH-dependent thioredoxin system constitutes a functional backup for cytosolic glutathione reductase in Arabidopsis. *Proc. Natl. Acad. Sci. U. S. A.* **106:**9109–9114; 2009.
[34] Braun, N. A.; Morgan, B.; Dick, T. P.; Schwappach, B. The yeast CLC protein counteracts vesicular acidification during iron starvation. *J. Cell Sci.* **123:**2342–2350; 2010.
[35] Sulston, J. E.; Horvitz, H. R. Post-embryonic cell lineages of the nematode, *Caenorhabditis elegans*. *Dev. Biol.* **56:**110–156; 1977.
[36] Hitchler, M. J.; Domann, F. E. An epigenetic perspective on the free radical theory of development. *Free Radic. Biol. Med.* **43:**1023–1036; 2007.
[37] Matthijssens, F.; Braeckman, B. P.; Vanfleteren, J. R. Evaluation of different methods for assaying protein carbonylation. *Curr. Anal. Chem.* **3:**93–102; 2007.
[38] Herndon, L. A.; Schmeissner, P. J.; Dudaronek, J. M.; Brown, P. A.; Listner, K. M.; Sakano, Y.; Paupard, M. C.; Hall, D. H.; Driscoll, M. Stochastic and genetic factors influence tissue-specific decline in ageing *C. elegans*. *Nature* **419:**808–814; 2002.
[39] Gerstbrein, B.; Stamatas, G.; Kollias, N.; Driscoll, M. In vivo spectrofluorimetry reveals endogenous biomarkers that report healthspan and dietary restriction in *Caenorhabditis elegans*. *Aging Cell* **4:**127–137; 2005.
[40] Masoro, E. J. Caloric restriction and aging: an update. *Exp. Gerontol.* **35:**299–305; 2000.
[41] Schulz, T. J.; Zarse, K.; Voigt, A.; Urban, N.; Birringer, M.; Ristow, M. Glucose restriction extends *Caenorhabditis elegans* life span by inducing mitochondrial respiration and increasing oxidative stress. *Cell Metab.* **6:**280–293; 2007.
[42] Avery, L.; Horvitz, H. R. Pharyngeal pumping continues after laser killing of the pharyngeal nervous system of *C. elegans*. *Neuron* **3:**473–485; 1989.
[43] Forrester, W. C.; Perens, E.; Zallen, J. A.; Garriga, G. Identification of *Caenorhabditis elegans* genes required for neuronal differentiation and migration. *Genetics* **148:** 151–165; 1998.
[44] Edens, W. A.; Sharling, L.; Cheng, G.; Shapira, R.; Kinkade, J. M.; Lee, T.; Edens, H. A.; Tang, X.; Sullards, C.; Flaherty, D. B.; Benian, G. M.; Lambeth, J. D. Tyrosine cross-linking of extracellular matrix is catalyzed by Duox, a multidomain oxidase/peroxidase with homology to the phagocyte oxidase subunit gp91phox. *J. Cell Biol.* **154:**879–891; 2001.
[45] Page, A. P. The nematode cuticle: synthesis, modification and mutants. Parasitic Nematodes. CABI, St Albans; 2001.
[46] Robertson, S. J.; Martin, R. J. The activation of nicotinic acetylcholine-receptors in the nematode parasite Ascaris-suum by the application of levamisole to the cytoplasmic surface of muscle membrane. *Pest. Sci.* **37:**293–299; 1993.

[47] Avery, L.; Horvitz, H. R. Effects of starvation and neuroactive drugs on feeding in *Caenorhabditis elegans*. *J. Exp. Zool.* **253:**263–270; 1990.
[48] Jackson, M. J. Reactive oxygen species and redox-regulation of skeletal muscle adaptations to exercise. *Philos. Trans. R. Soc. Lond. B Biol. Sci.* **360:**2285–2291; 2005.
[49] Rogers, J. M.; Hunter III, E. S. Redox redux: a closer look at conceptal low molecular weight thiols. *Toxicol. Sci.* **62:**1–3; 2001.
[50] Beck, M. J.; McLellan, C.; Lightle, R. L.; Philbert, M. A.; Harris, C. Spatial glutathione and cysteine distribution and chemical modulation in the early organogenesis-stage rat conceptus in utero. *Toxicol. Sci.* **62:**92–102; 2001.
[51] Kubagawa, H. M.; Watts, J. L.; Corrigan, C.; Edmonds, J. W.; Sztul, E.; Browse, J.; Miller, M. A. Oocyte signals derived from polyunsaturated fatty acids control sperm recruitment in vivo. *Nat. Cell Biol.* **8:**1143–1148; 2006.